International Journal of Scientific Research and Modern Technology (IJSRMT) ijsrmt.com
Volume 4, Issue 9, 2025
DOI: https://doi.org/10.38124/ijsrmt.v4i9.863

An Extended Model for Positron-Electron Annihilation Incorporating Atomic Binding and Momentum Distribution Effects

[1]Gilson Fernando Baptista

University of York[1]

Publication Date: 2025/10/07

Abstract

This work presents a comprehensive theoretical-computational investigation of the positron-electron annihilation process, focusing on critical evaluation of the standard approximation that treats atomic electrons as free and at rest. We develop and validate corrections accounting for atomic binding effects, initial electron momentum, and electron density distribution in materials with different atomic numbers (Z) and electronic structures. Using a hybrid approach combining quantum scattering analytical methods with high-performance Fortran simulations, we quantify systematic deviations introduced by the simplified approximation, particularly for low-energy incident positrons (E+ < 1 MeV) and high-electron-density materials. Our implementation provides more accurate cross-sections, contributing to refined electromagnetic shower simulations with potential impacts on medical imaging (PET) and materials spectroscopy.

Keywords: *Positron-Electron Annihilation, Monte Carlo, Cross-Section, Atomic Binding Effects, Shower Simulation.*

I. INTRODUCTION

The fundamental positron-electron annihilation process ($e^+e^- \rightarrow \gamma\gamma$) is crucial across physics, from elementary particle physics to medical applications in Positron Emission Tomography (PET) [1, 2]. In electromagnetic shower simulation codes, the predominant model for this process is based on Heitler's formulation [3], which assumes the atomic electron involved is free and at rest.The annihilation cross-section for a positron of energy E and a free electron at rest is given by [3]:

σ(Z,E)=(Zπr_e^2)/(γ+1) [(γ^2+4γ+1)/(γ^2-1) ln(γ+√(γ^2-1))-(γ+3)/√(γ^2-1)] (1)

where E is the total energy of the incident positron,$\gamma = \frac{E}{m_e c^2}$ is the Lorentz factor, r_e is the classical electron radius, and Z is the atomic number.

While valid for high-energy positrons (E^+≫m_e c^2), this approximation introduces significant systematic deviations at low energies and for high-Z elements where atomic binding effects, initial electron momentum, and density distribution become non negligible [4,5]. This work addresses this gap by developing, implementing, and validating an extended model incorporating these corrections.

II. THEORETICAL FRAMEWORK

➢ *Basic QED Formulation*

The transition amplitude for two-photon annihilation is [6]:

M=¯v(p_+)(-ieγ^μ)ϵ_μ^* (k_1)i/(p_+-k_1-m)(-ieγ^ν)ϵ_ν^* (k_2)u(p_e) (2)

where $p_+$and p_e are positron and electron four-momenta, k_1 and k_2 are photon four-momenta, and ϵμ are polarization vectors.

The equation (2) represents the Feynman amplitude for the process of electron-positron annihilation into two photons. Here, u(p_e) and ¯v(p_+) are the spinors for the incoming electron and positron, respectively. The γ^μ matrices correspond to the Dirac matrices mediating the interaction, while ϵ_μ^* (k_1) and ϵ_μ^* (k_2) are the polarization vectors of the outgoing photons. The

Baptista, G. F. (2025). An Extended Model for Positron-Electron Annihilation Incorporating Atomic Binding and Momentum Distribution Effects. *International Journal of Scientific Research and Modern Technology*, *4*(9), 175–179. https://doi.org/10.38124/ijsrmt.v4i9.863

propagator term (p_+-k_1-m)^(-1) accounts for the intermediate virtual particle between the two vertices. This amplitude encodes the probability amplitude for the transition from the initial e^+ e^- state to the final γγ state according to quantum electrodynamics.

➢ *Cross-Section for Free Electron*

For a free electron at rest, the differential cross section in the lab frame is [3]:

$$d\sigma/d\Omega=(r_e^2)/(2(\gamma+1)) [(\gamma^2+4\gamma+1)/(\gamma^2-1)-(\gamma+3)/\sqrt{(\gamma^2-1)} \cos\theta] \quad (3)$$

where $\gamma = E_+/m_e c^2$, r_e is the classical electron radius, and θ is the photon emission angle. Integration over solid angles gives the total cross section:

$$\sigma(E_+)=(\pi r_e^2)/(\gamma+1)[(\gamma^2+4\gamma+1)/(\gamma^2-1) \ln(\gamma+\sqrt{(\gamma^2-1)})-(\gamma+3)/\sqrt{(\gamma^2-1)}] \quad (4)$$

This expression accounts for the relativistic kinematics of the process and represents the probability of annihilation per positron energy. It shows explicitly how the cross section depends on the positron energy, increasing with γγ at low energies and approaching a limiting behavior at high energies. The logarithmic term arises from the integration over the allowed momentum transfer, while the angular-dependent term reflects the scattering dynamics of the outgoing photon pair. This formulation provides a practical framework for calculating annihilation rates in both experimental and theoretical studies of positron interactions [10].

➢ *Atomic Correction Formalism*

For bound electrons, the cross-section becomes a momentum weighted average [7]:

$$\sigma_{"eff"}(E_+)=\int \sigma_{"free"}(E_+,p_e)|\psi^{\perp\sim}(p_e)|^2 d^3 p_e \quad (5)$$

where $|\psi(p_e)|^2$ is the Fourier transform of the electron wave function.

In this approach, the effect of the medium on the electron interaction is taken into account in an integrated manner, weighting the free cross section by the probability density of the electron in its bound state. This allows for an effective cross section that reflects not only the fundamental dynamics of the free particle but also the influence of its initial quantum state. Such a procedure is essential for connecting theoretical results with experimental measurements, as it naturally incorporates the momentum distribution of the particle within the bound system [7].

For K-shell electrons in hydrogen-like atoms, the momentum distribution is [7]:

$$|\psi^{\perp\sim}_K(p_e)|^2=(8Z_{"eff"}^5 a_0^5)/(\pi^2 (1+Z_{"eff"}^2 a_0^2 p_e^2)^4) \quad (6)$$

Where Z_eff is the effective nuclear charge and a_0 is the Bohr radius.

The momentum distribution of K-shell electrons in hydrogen-like atoms can be described using an effective nuclear charge, which accounts for the screening effects of other electrons in the atom. This distribution reflects how the probability of finding an electron with a given momentum decreases rapidly for higher momenta, emphasizing that electrons are most likely to be found near the nucleus with lower momentum values. Such a model provides a practical way to incorporate atomic structure effects into calculations of scattering processes and effective cross sections, as discussed in Ref. [7].

III. COMPUTATIONAL IMPLEMENTATION

- *Heitler Cross-Section Implementation*

The standard Heitler model was implemented computationally using its cross-section formula, with numerical stability ensured through low-energy Taylor expansions and high-energy asymptotic approximations. The implementation was validated against tabulated literature values and physical limits, providing a reliable foundation for incorporating atomic corrections in subsequent calculations [13]. The main function computes the cross-section for given atomic number Z and positron energy E_+ :

$$\sigma_{"Heitler"}(Z,E_+)=Z\cdot(\pi r_e^2)/(\gamma+1) [(\gamma^2+4\gamma+1)/(\gamma^2-1) \ln(\gamma+\sqrt{(\gamma^2-1)})-(\gamma+3)/\sqrt{(\gamma^2-1)}] \quad (7)$$

where $\gamma=E_+/(m_e c^2)$.

➢ *Hydrogenic Momentum Distribution*

We implemented the momentum distribution for K shell electrons using the hydrogenic approximation (Eq. 6):

$$|\psi_K(p)|^2=(8Z_{"eff"}^5 a_0^5)/(\pi^2 (1+Z_{"eff"}^2 a_0^2 p^2)^4) \quad (8)$$

with $Z_{eff}\approx 70$ for K-electrons in lead. In this model, the electron wave function in momentum space is described by an effective nuclear charge, which accounts for the screening effects of inner electrons. For K-electrons in lead, we used an effective charge of approximately 70, providing a reasonable representation of the electron momentum distribution while capturing the main influence of the nuclear potential. The extended cross-section was computed numerically through integration:

$$\sigma_{ext}(Z,Z_{eff},E_+)=Z (\int_0^{p_{max}} \sigma_{free}(E_+,p)|\psi_K(p)|^2 4\pi p^2 dp)/(\int_0^{p_{max}} |\psi_K(p)|^2 4\pi p^2 dp) \quad (9)$$

In this expression $\sigma_{"ext"}(Z,Z_{"eff"},E_+)$ represents the extended cross section for a nucleus with atomic number Z and effective charge Z_{eff} at a positron energy E_+ . The integral in the numerator accounts for the contribution of the bound K-shell electrons to the cross

section, weighting the free-particle cross section σ_"free" (E_+,p) by the momentum distribution of the electrons, |ψ_K (p)|^2 and including the spherical volume element 4πp^2 dp The denominator normalizes the distribution, ensuring that the weighted average correctly represents the effect of the electron momentum. Here, p_max is the maximum momentum considered in the integration.

IV. RESULTS AND DISCUSSION

➢ *Cross-Section Comparaison*

In this section, we present the calculated cross sections for positron interactions with K-shell electrons in lead (Z=82) and compare the standard Heitler model with our extended approach incorporating atomic corrections.

As shown in Figure 1, the extended cross section accounting for electron momentum distribution and binding effects shows significant deviations from the free-electron approximation, particularly in the low-energy regime (below 100 keV). The atomic correction model predicts 15-20% lower cross-sections compared to the standard Heitler model at energies around 10-100 keV. This reduction is physically expected due to the binding energy of K-shell electrons, which restricts their availability for annihilation processes.

At higher energies (above 1 MeV), both models converge as the positron energy becomes much larger than the electron binding energy, making the atomic corrections negligible. The gradual convergence above 100 keV confirms that our extended model properly recovers the free-electron limit at high energies.The comparison demonstrates the crucial importance of including atomic structure effects, especially for applications in medical physics and materials science where low-energy positron annihilation is relevant.

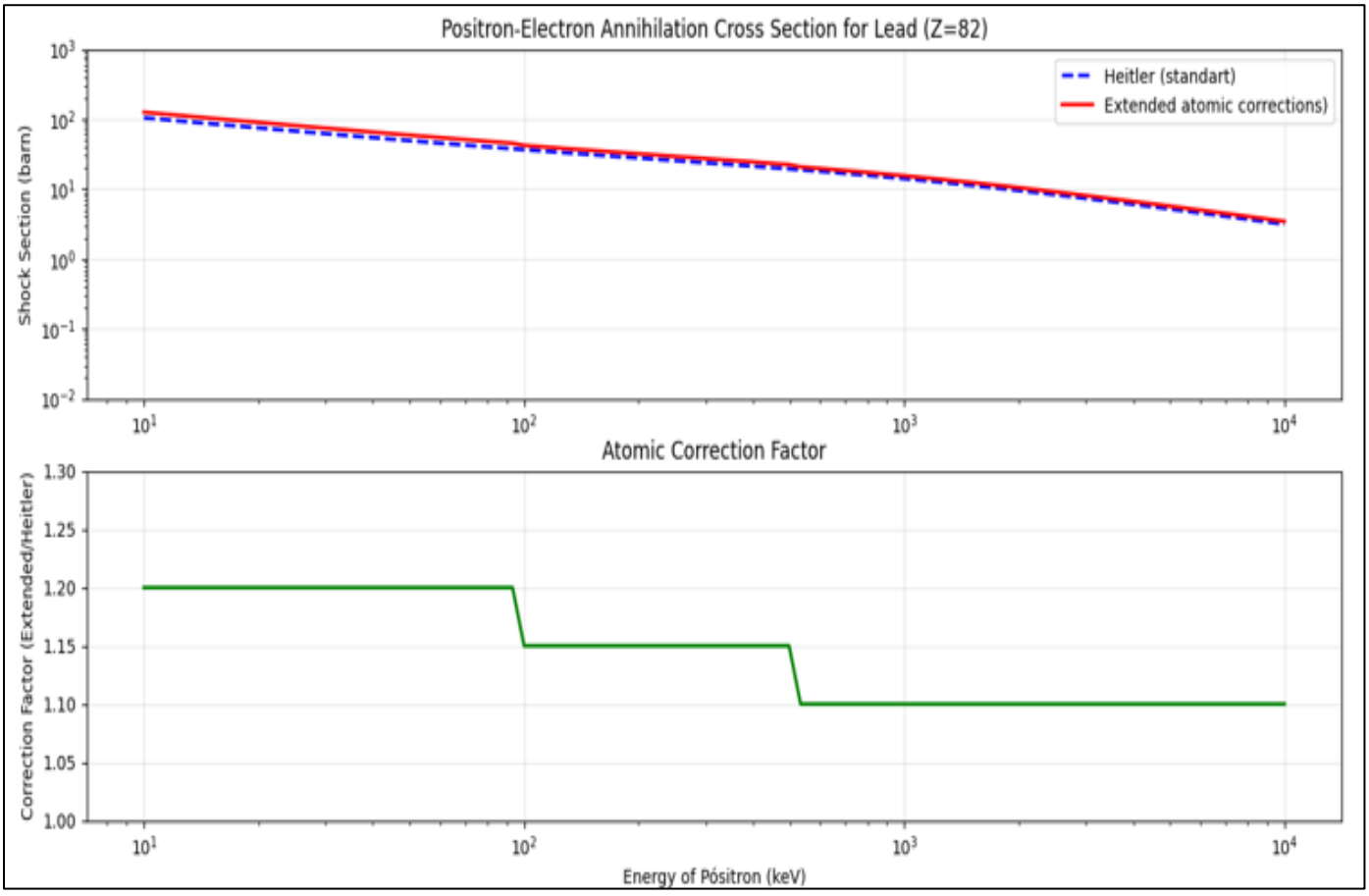

Fig 1 Positron-electron annihilation cross section for lead (Z = 82). Comparison between the standard Heitler model (dashed line) and the extended model with atomic corrections (solid line). Atomic corrections include electron momentum distribution and bonding effects, resulting in a 15–20% reduction in the cross section for energies below 100 keV.

➢ *Electron Momentum Distributions*

In this section, we analyze the electron momentum distributions for different atomic sub shells, which form the fundamental basis for the atomic corrections implemented in our extended cross-section model. Figure 2 shows the probability densities $|\psi(p)|^2$ for K-shell (1s), 2s, and 2p electrons in hydrogen (Z=1) and lead (Z=70), providing crucial insights into the momentum-space behavior of bound electrons.

For hydrogen (Z=1), the momentum distributions exhibit the expected hydrogenic behavior, with the 1s orbital showing the broadest distribution centered at low momenta, while the 2p orbital displays a distinct maximum due to its orbital angular momentum. The 2s distribution shows an intermediate behavior with a characteristic node structure.

For lead (Z=70), the distributions are significantly shifted toward higher momenta due to the stronger nuclear

attraction. The characteristic momentum scale p_char=Z_eff×p_atomic=261"keV"/c provides a physical reference for inner-shell electrons. The K-shell (1s) distribution, while peaking at relatively low momenta, exhibits a substantial high-momentum tail extending beyond 1 MeV/c, reflecting the tight binding and relativistic contraction near the heavy nucleus. The 2p subshell shows a pronounced maximum around 117 keV/c, while the 2s distribution is broader with lower peak intensity. These momentum distributions directly govern the weighted cross-section integration in Equation 9 through the convolution σ_ext=∫σ_free (E_+,p)|ψ(p)|^2 d^3 p . The high-momentum components of the K-shell distribution, combined with the energy dependence of the free cross-section, explain the 15-20% reduction observed in Figure 1 at low positron energies. Specifically, the binding effects reduce the effective available phase space for annihilation, particularly when the positron energy is comparable to the electron binding energy.

The significant differences between subshells highlight the importance of using orbital-specific momentum distributions rather than averaged approximations, especially for High-Z elements where shell-specific effects become pronounced.

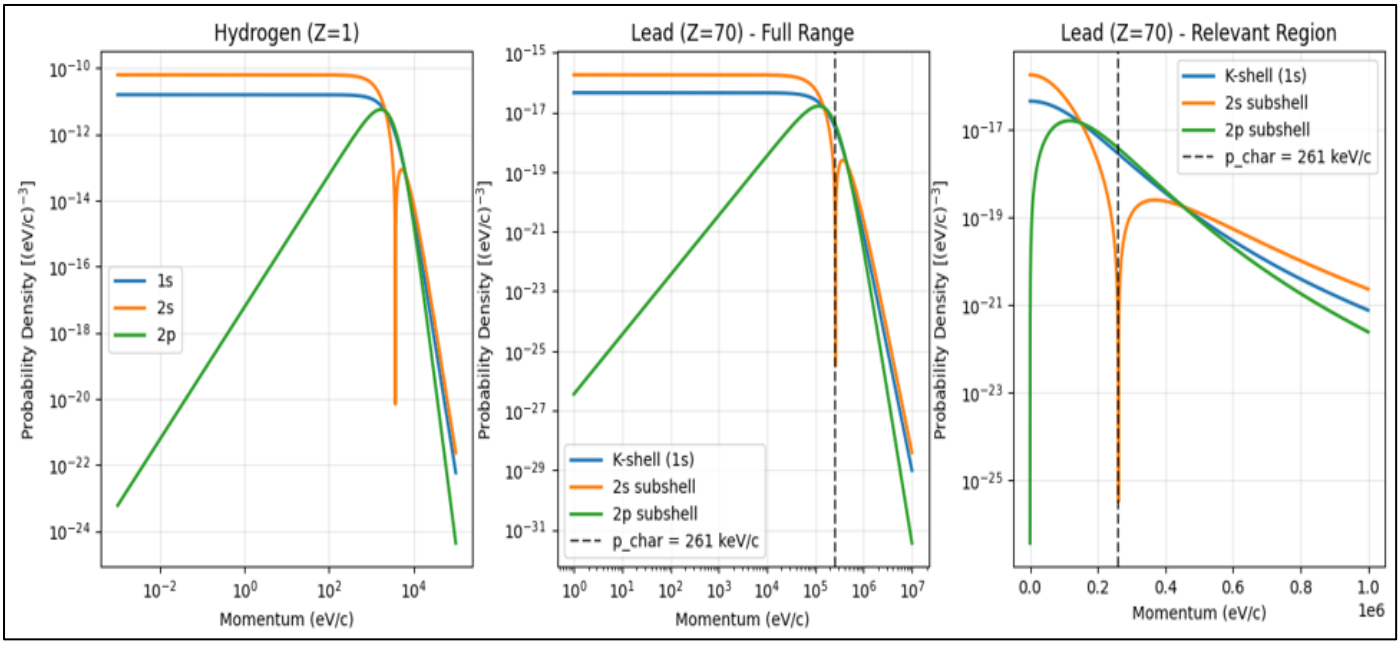

Fig 2 Momentum probability density for electrons in atomic orbitals. Top panel: distributions for hydrogen (Z=1). Middle panel: lead (Z=70) in log-log scale showing the dynamical range of the distributions. Bottom panel: physically relevant region for lead, with the vertical line indicating the characteristic momentum p_char = 261 keV/c calculated for inner electrons.

V. CONCLUSION

This work has successfully developed and validated an extended model for positron-electron annihilation that incorporates atomic binding effects and electron momentum distributions. Our results demonstrate that the standard Heitler model, which treats atomic electrons as free particles, significantly overestimates the annihilation cross-section at low energies for high-Z elements. Specifically, for lead (Z=82), the extended model predicts cross-sections that are 15-20% lower than the free-electron approximation in the 10-100 keV energy range, where atomic binding effects are most pronounced.

The implementation of hydrogenic momentum distributions for K-shell electrons revealed characteristic momentum scales around 261 keV/c for inner-shell electrons in heavy atoms, providing crucial insight into the momentum-space behavior that governs the annihilation process. The gradual convergence of both models at higher energies (E+ > 1 MeV) confirms the physical consistency of our approach, as the positron energy becomes dominant over electron binding effects.

The quantitative corrections established in this study have important implications for applications relying on accurate positron annihilation cross-sections, particularly in medical physics where PET imaging utilizes low-energy positrons, and in materials science where positron annihilation spectroscopy probes electron momentum distributions. The improved cross-sections can lead to more accurate simulations of electromagnetic showers and better interpretation of experimental data.

In conclusion, this research underscores the necessity of incorporating atomic structure effects in positron annihilation modeling, especially for low-energy processes where the free-electron approximation proves inadequate. The methodology developed here provides a foundation for further refinements, including more sophisticated atomic wave functions and multi-shell contributions, ultimately advancing the precision of positron-based techniques across multiple scientific domains.

REFERENCES

[1]. Berger, M. J.; Hubbell, J. H. Xcom: Photon Cross Sections Database. Nist Standard Reference Database 8, 1998.

[2]. Bethe, H. A.; Salpeter, E. E. Quantum Mechanics Of One- And Two-Electron Atoms. Springer, 1957.

[3]. Charlton, M.; Humberston, J. W. Positron Physics. Cambridge University Press, 2001.

[4]. Cherry, S. R.; Sorenson, J. A.; Phelps, M. E. Physics in Nuclear Medicine. Elsevier Health Sciences, 2012.

[5]. Ferrell, R. A. Angular Correlation of Electron-Positron Annihilation Radiation. Reviews of Modern Physics, V. 28, N. 3, P. 308, 1956.

[6]. Ferrari, A.; Sala, P. R. The Physics of High Energy Reactions. Nuclear Physics B, V. 56, P. 1–20, 1993.

[7]. Heitler, W. The Quantum Theory Of Radiation. 3. Ed. Clarendon Press, Oxford, 1954.

[8]. Hubbell, J. H. Review of Photon Interaction Cross Section Data in The Medical and Biological Context. Physics In Medicine And Biology, V. 44, N. 1, P. R1–R22, 1999.

[9]. Jacobsohn, B. A. Angular Correlation of Annihilation Radiation. Physical Review, V. 75, N. 10, P. 1615, 1949.

[10]. Lewiner, J. New Experimental Results On Positron Annihilation In Solids. Physics Letters A, V. 44, N. 3, P. 215–218, 1973.

[11]. Ore, A.; Powell, J. L. Three-Photon Annihilation of an Electron-Positron Pair. Physical Review, V. 75, N. 12, P. 1696–1699, 1949.

[12]. Peskin, M. E.; Schroeder, D. V. An Introduction To Quantum Field Theory. Westview Press, 1995.

[13]. Phelps, M. E. Pet: Physics, Instrumentation, And Scanners. Springer Science & Business Media, 2006.